Current Research in Food Science 9 (2024) 100941

Contents lists available at ScienceDirect

Current Research in Food Science

journal homepage: www.sciencedirect.com/journal/current-research-in-food-science

Improving gel properties of egg white protein using coconut endosperm dietary fibers modified by ultrasound and dual enzymolysis combined with carboxymethylation or phosphate crosslinking

Anyu Zhang [a,1], Jun Ma [b,c,d,1], Peiyao Long [a], Yajun Zheng [a,*], Yichan Zhang [a]

[a] Food Science College of Shanxi Normal University, Taiyuan, 030092, China
[b] Shanxi Province Cancer Hospital, Taiyuan, 030013, China
[c] Shanxi Hospital Affiliated to Cancer Hospital, Chinese Academy of Medical Sciences, Taiyuan, 030013, China
[d] Cancer Hospital Affiliated to Shanxi Medical University, Taiyuan, 030013, China

ARTICLE INFO

Handling Editor: Dr. Xing Chen

Keywords:
Coconut endosperm fiber
Ultrasonic
Dual enzymatic hydrolysis
Crosslinking
Carboxymethylation
Egg white protein gel

ABSTRACT

Coconut endosperm residue is a rich dietary fiber resource; however, its hydration properties are poor. To enhance the functionality and applications of coconut endosperm residue dietary fiber (CERDF) in the food industry, ultrasound, cellulase, and hemicellulase hydrolysis combined with carboxymethylation or phosphate crosslinking have been used. The impact of the modified CERDFs on egg white protein gel (EWPG) was also studied. Compared to unmodified CERDF, CERDF modified by ultrasound and dual enzymatic hydrolysis combined with carboxymethylation (CERDF-UDEC) or phosphate-crosslinking (CERDF-UDEPC) exhibited a larger surface area and improved water retention and expansion abilities ($p < 0.05$). Addition of CERDF, CERDF-UDEC, and CERDF-UDEPC increased the random coil content of EWPG and rendered its microstructure more granular. CERDF-UDEC and CERDF-UDEPC improved EWPG properties more effectively than unmodified CERDF. These enhancements included increased water retention, pH, hardness (from 109.87 to 222.38 g), chewiness (from 78.07 to 172.13 g), and gumminess (from 85.12 to 181.82), and a reduction in its freeze-thaw dehydration rate (from 33.66% to 16.26%) and transparency ($p < 0.05$). Adding CERDF and CERDF-UDEC (3–5 g/100 g) enhanced the gastric stability and intestinal digestibility of EWPG. Thus, CERDF modified through ultrasound and dual enzymolysis combined with carboxymethylation or crosslinking improved the gel properties of EWPG. However, further research is needed to clarify the mechanisms behind these modifications and evaluate their economic feasibility.

1. Introduction

Hydrophilic macromolecules, such as proteins and polysaccharides, can interact with water to form hydrogels, which are extensively used in food, medicine, cosmetics, and other industries (Alavi et al., 2020; Farahani, 2021). Protein-based hydrogels, especially egg white protein gel (EWPG), have garnered considerable attention due to their biocompatibility, biodegradability, and ease of modification (Kar et al., 2023). Under the influence of certain inducible factors, such as heating, alkali, acid, and salt, egg white proteins can interact to form a gel structure. Heat-induced egg white protein gel has unique texture properties such as high elasticity, springiness, and chewiness, but their hardness, gumminess, water-retention ability, and freeze-thaw properties are poor (Zang et al., 2023; Lv et al., 2022). Moreover, EWPG's high transparency limits their application in the preservation of photosensitive foods. Studies have shown that a mixture of egg white protein and polysaccharides can offer better gel properties than egg white proteins alone and that hydrophilic polysaccharides can effectively improve the texture quality of EWPG (Farahani et al., 2022a; Farahani et al., 2023a; Liu et al., 2022; Xiao et al., 2020). Dietary fiber, a low- or no-calorie polysaccharide with functionalities, such as reduced hypertension, diabetes, obesity, gastrointestinal inflammation, and cancer (Lv et al., 2022). Some soluble dietary fibers (SDF) such as pectin, gum, and inulin have good gel properties (Grootaert et al., 2022; Farahani et al., 2023b; Farahani et al., 2022b). The textural quality and functional properties of EWPG improves fortification with dietary fibers

* Corresponding author. Shanxi Normal University, Taiyuan, 030092. China
E-mail address: zyj_coconut@163.com (Y. Zheng).
[1] The two authors contribute equally to this work.

https://doi.org/10.1016/j.crfs.2024.100941
Received 30 August 2024; Received in revised form 18 November 2024; Accepted 29 November 2024
Available online 30 November 2024

(Xiao et al., 2020; Ullah et al., 2019), however, research on the effect of dietary fibers on EWPG is limited.

The physicochemical characteristics of dietary fiber, especially its gel properties, are positively correlated with its SDF content. Dietary fiber with an SDF content exceeding 10 g/100 g is classified as high quality (Zhao et al., 2023; Gan et al., 2021). Dietary fibers can be found in oil crop byproduct which are inexpensive and widely available. Oil crop byproduct, contain low SDF content, generally below 4 g/100 g (Huyst et al., 2022). Consequently, modification methods to convert insoluble dietary fiber (IDF) to SDF have been studied extensively. These modifications can alter the size, microstructure, functional groups, and physicochemical properties of dietary fiber through physical, chemical, or biological methods (Gan et al., 2021; Dong et al., 2022; Kanwar et al., 2023; Tian et al., 2024). However, studies on the combined effect of physical, chemical, and biological methods for converting IDF to SDF remain scarce.

The coconut (*Cocos nucifera* L.) is an important woody oil crop in tropical and subtropical region. Coconut milk and oil are produced from coconut endosperm via wet and dry processing procedures, respectively, both of which generate large amounts of coconut endosperm residue (CER) (Adeloye et al., 2020; Begum et al., 2024). Recently, owing to the increasing demand for coconut oil and milk in the global market, the yield of CER has increased. CER is an abundant, low-cost, and under-exploited resource of insoluble dietary fiber (Tan et al., 2022). Although previous studies have shown that coconut endosperm residue dietary fiber (CERDF) has high water expansion and oil-adsorbing abilities, its applications in food industry are limited, mainly due to its low soluble fiber content and poor hydration properties (Trinidad et al., 2006; Zheng and Li, 2018; Hanafi et al., 2022). To enhance the physicochemical and functional properties of CERDF, several methods such as high-pressure homogenisation, cellulase hydrolysis, hydroxypropylation, and carboxymethylation have been employed in the last decades (Nansu et al., 2019; Zheng et al., 2021; Gao et al., 2023). Tian et al. (2024) found that ultrasound significantly improves the glucose and salt adsorption capacities of coconut residue fiber. The effects of carboxymethylation, crosslinking, and enzymolysis on the hydration properties of CREF have been verified by Zheng et al. (2021) and Nansu et al. (2019). A combination of ultrasound, enzymatic hydrolysis and these chemical methods may be in improving the functional properties of CERDF; however, relevant data are scare. Therefore, the current study investigates the effects of ultrasound, cellulase, and hemicellulase hydrolysis, each combined with carboxymethylation and phosphate crosslinking, on the structural and hydration characteristics of CREDF; and examines the influence of modified CERDF on the gel properties of EWPG. This study provides new, effective ways with promising application prospects for improving the functional characteristics of dietary fiber and gel properties of EWPG.

2. Materials and methods

2.1. Materials

Coconut (*Cocos nucifera* L.) endosperm residue (produced on May 12th, 2024) was purchased from Shengxing Coconut Trading Co., Ltd., Guangzhou, China. Egg white protein powder (protein content above 95%) was purchased from Zhongji Egg Co., Ltd., (Hebi, China). Cellulase (from *Aspergillus niger*, 5.0×10^5 U/g), hemicellulase (from *Trichoderma Vride G*, 1.5×10^4 U/g), α-amylase (from *Bacillus licheniformis*, 1.0×10^5 U/g), pepsin (from porcine stomach mucose), and trypsin (from bovine pancreas, 1: 250 U/mg) were from Yigao Reagent Co., Ltd., Wuhan, China. Analytical-grade propylene oxide, thiosalicylic acid, and sodium chloride were purchased from Daimiao Chemical Reagent Factory (Tianjin, China).

2.2. Extraction and ultrasonic treatment of CERDF

CERDF was extracted from coconut endosperm residue following the method described by Zheng and Li (2018). Briefly, coconut endosperm residue was dried and defatted using petroleum ether (boiling point range of 60–90 °C) in triplicates. Afterwards, α-amylase (1:100, g/g, enzyme to coconut endosperm residue), Alcalase (8:1000, enzyme to coconut endosperm residue, g/g), and glucoamylase (8: 1000, enzyme to coconut endosperm residue, g/g) were sequentially to remove starches, proteins, and soluble carbohydrates from the defatted coconut endosperm residue. Afterwards, the extraction solution was discarded and the residue was washed with deionised water and air-dried in a GFGZ-II blast drying oven (Zhuji Dry Instrument Factory, Shaoxing, China) at 52 °C for 8 h, and then CERDF was obtained. Next, CERD (20 g) and 260 mL of phosphate buffer (pH 4.5, 0.1 mol L^{-1}) were added to a glass flask, mixed thoroughly, and treated using an XU-UP-400 ultrasonic cell crusher (Yuze Technology Co., Ltd., Jining, China) at 400 W to obtain ultrasonically treated coconut endosperm residue dietary fiber (CERDF-U) (Liu et al., 2021).

2.3. Dual enzymatic treatment of CERDF-U

Citing the method from Zheng & Li (Zheng and Li, 2018), hemicellulase (0.8 g) and cellulase (0.64 g) were added to a CERDF dispersion (40 g CERDF were dispersed in 600 mL of deionised water), which was shaken at 50 °C, 205 rpm and pH 5.0 for 150 min. The reaction was terminated via heating treatment (100 °C, 10 min). After cooling and filtration, the residue on the filter paper was dehydrated at 45 °C in the GFGZ-II blast drying oven. After 6 h, the ultrasound and dual enzyme-treated coconut endosperm residue dietary fiber (CERDF-UDE) were obtained.

2.4. Carboxymethylation of CERDF-UDE

CERDF-UDE (8 g) was dispersed in 80 mL of ethanol (85%, v/v) with magnetic stirring at 300 rpm for 30 min (Zheng et al., 2021). Simultaneously, sodium hydroxide solution (1.13 mol L^{-1}, 10 mL) was mixed with 40 mL of ethanol (85%, v/v) at 215 rpm and 35 °C for 45 min, and then added to the CERDF-UDE dispersion, stirred at 300 rpm and 35 °C for 65 min. Next, sodium hydroxide solution (3.38 mol L^{-1}, 40 mL) and chloroacetic acid (3.38 mol L^{-1}, 20 mL) were added to the reaction dispersion. After stirring at 300 rpm and 53 °C for 210 min, the reaction mixture was cooled and adjusted to pH 7.0 using acetic acid (50%, v/v), and then filtered using Whatman 1007-04B paper. The residue was collected and washed thrice with anhydrous ethanol (60 mL). After drying at 48 °C for 12 h, the CERDF modified by ultrasound, and dual enzymolysis and carboxymethylation (CERDF-UDEC) was obtained.

2.5. Crosslinking of CERDF-UDE

CERDF-UDE (10 g), sodium tripolyphosphate (0.24 g) and sodium trimetaphosphate (2.4 g) were dispersed in 100 mL deionised water (dH_2O), and the pH value was adjusted to 11.0 using 1 mol L^{-1} of NaOH (Hazarika and Sit, 2016). The mixture was stirred at 300 rpm and 45 °C for 180 min. The reaction was then stopped by adjusting the pH to 7.0 using HCl (1 mol L^{-1}). After filtration, the residue was collected, washed using dH_2O (80 mL). CERDF, modified by ultrasound, dual enzymatic hydrolysis, and phosphate crosslinking (CERDF-UDEPC), was obtained after drying at 40 °C overnight.

2.6. Preparation of egg white protein gels

Fifteen grams of egg white powder was dissolved in 100 mL dH_2O and stored at 4 °C overnight. The egg white solution (20 mL) was transferred into a 50 mL beaker, and CERDF, CERDF-UDEC, CERDF-UDEA, or CERDF-UDEPC in varying amounts (1, 2, 3, 4, and 5 g/100 g)

was added. The mixture was gently stirred using a BHE-002Z shaker at 90 °C for 30 min. This process included two stages: stirring at 160 rpm for 3 min, and holding for 27 min at 0 rpm (Hazarika and Sit, 2016). Finally, the mixtures were cooled and stored at 4 °C for 7 h to get heat-induced egg white gel (EWPG), and heat-induced egg white gels separately fortified with CERDF (EWPG/CERDF), CERDF-UDEC (EWPG/CERDF-UDEC), CERDF-UDEPC (EWPG/CERDF-UDEPC), and CERDF-UDEA (EWPG/CERDF-UDEA).

2.7. Chemical constituents, surface area and colour determinations

The soluble, insoluble, and total dietary fiber contents of CERDF, CERDF-UDEC, CERDF-UDEA, and CERDF-UDEPC were determined using the AOAC.991.43 method (AOAC, 2000) (AOAC, 2000). AOAC.955.04, AOAC.920.39, AOAC.924.05 and AOAC.92.05 were separately employed to analyse the ash, protein, moisture, and fat contents of the CERDFs (AOAC, 2000). Moreover, the AOAC.991.43 method was employed to determine the insoluble and total fiber contents; the soluble fiber content was the difference between the total fiber and insoluble fiber contents (AOAC, 2000). The surface area ($m^2 \bullet kg^{-1}$) and particle size (Sauter mean diameter, $D_{3,2}$) were analysed with a JFNER-LB particle size analyser (Jingbei Frontier Instrument Co., Chengdu, China). The colour indices, including L (indicative of lightness), b (representative of redness), and a (corresponding to yellowness), were determined using an NH130 High Quality Portable Colour Difference Meter (Three-NH Colorimeter Co., Shenzhen, China). Colour differences (ΔE) across CERDF and modified CERDFs (fortified with CERDFs) were calculated as follows:

$$\Delta E = \sqrt{(L - L_0)^2 + (a - a_0)^2 + (b - b_0)^2} \quad (1)$$

where a_0, L_0, and b_0 denote the redness, lightness, and yellowness of untreated CERDF, respectively.

2.8. Structural investigations

2.8.1. Scanning electron microscopy

First, CERDFs and EWPGs were coated with a 10 nm gold layer. The samples were scanned using a scanning electron microscope (SEM; JOLE-JMS-5700E, Tokyo, Japan). The accelerating voltage, scale bar, and magnification were 5 kV, 1 μm, and 5,000, respectively (Farahani et al., 2024a).

2.8.2. Fourier-transformed infrared spectroscopy

The CERDFs and EWPGs were freeze-dried using a vacuum freeze-dryer (HFD-6, Heyuan Ice Equipment Co., LTD, Zhengzhou, China) and were then scanned using a Fourier-transform infrared (FT-IR) spectrometer (8400S, Shimadzu, Japan) at a resolution of 4 cm^{-1} and wavenumber scope of 4000–400 cm^{-1}. PeakFit software v4.12 (Seasolve, Framingham, MA, USA) was used to analyse the secondary structure of the EWPGs, using the procedure described by Bashash et al. (2022).

2.9. Water-retention and expansion abilities and viscosity

The water expansion ability (WEA) and water holding ability (WHA) of the samples were determined using the procedures described by Farahani and Mousavi (Farahani et al., 2024b). The viscosity of the CERDFs was measured according to the procedure described by Farahani et al. (2022c) using a RAV-I5 viscometer (Shengyebao Niandu Instrument Factory, Guangzhou, China).

2.10. Characterization of gels

2.10.1. Water-holding ability of gels

Centrifugation was performed to determine the WHA of the gel samples (Zheng et al., 2022). Briefly, in a centrifuge tube (50 mL), approximately 2 g (M_0) of EWPGs was added, along with a filter paper. After centrifugation at 4000×g at 4 °C for 20 min, the gel samples were weighed again (M_1). WHA (%) was calculated as follows:

$$\text{WHA}\ (\%) = M_1 / M_0 \times 100\% \quad (2)$$

where M_0 and M_1 represent the gel weights before and after centrifugation, respectively.

2.10.2. Freeze-thaw cycle test

The gel samples were loaded into a 15 mL glass centrifuge tubes for syneresis measurements (Khemakhem et al., 2019). The freeze-thaw cycle contained two steps: (1) the gels in the tube were frozen at −16 °C for 24 h; and (2) the frozen gels were slowly thawed at room temperature (approximately 25 °C) for 8 h. The gel was subjected to such cycles and was weighed (W_s). After filtration (3500×g, 15 min), the weight of the residue was measured and recorded as W_d. The dehydration rate in the freeze-thaw cycle was quantified according to Equation (3):

$$\text{Dehydration rate}\ (\%) = (W_s - W_d) / W_s \times 100\% \quad (3)$$

2.10.3. Optical transparency of gel

The gel sample was transferred to a quartz colorimetric dish and its absorbance was determined using a JH754PC UV–Vis spectrophotometre (Shanghai Jinghua Co., Ltd., China) at 600 nm (Hou et al., 2022).

2.10.4. Textural properties

The textural properties of EWPGs, including hardness, elasticity, cohesiveness, adhesiveness, chewability, and resilience, were measured using a TA Plus Texture Analyser System (LLOYD Instrument Co., HK) with a P/36 R probe. Data were measured in the TPA mode, and the test parameters were as follows: trigger force, compression rate, and test, pre-test, and post-test speeds of 5 g, 50%, 1, 2, and 1 mm/s, respectively (Hou et al., 2022; Farahani and Mousavi, 2023).

2.11. In vitro gastrointestinal digestions

The *in vitro* gastrointestinal digestion of EWPGs was performed according to the procedures described by Lee et al. (2024). The simulated gastric fluid (pH 2.0) was prepared by mixing NaCl (2 g/L), pepsin (4000 U/mL) and HCl (0.1 mol/L), and the intestine digest fluid (pH 7.0) was consisted of trypsin (800 U/mL), bile salt (1 g/100 mL), NaCl (0.8775 g/100 mL), and K_2HPO_4 (0.68 g/100 mL). In a conical flask, the EWPGs (4 g) were crushed, mixed with 20 mL of simulated gastric fluid, and then shaken at 120 rpm and 37 °C for 1 h to simulate gastric digestion stage. Next, the mixture was adjusted to pH 7.0, and 20 mL of simulated intestinal fluid was added and shaken at 160 rpm and 37 °C for 2 h. During the entire digestion process, equivalent digestive juice (1 mL) was removed per 0.5 h for free amino acid content determination, and the reaction solution was kept at the same volume by adding the corresponding digestive fluid. The o-phthalaldehyde (OPA) assay was used to quantify the free amino acid content of the transferred digestive juice (Church et al., 1983). The OPA reagent contained sodium dodecyl sulfate (10 g$\bullet$100 mL^{-1}, 5 mL), β-mercaptoethanol (200 μL), sodium tetraborate (50 mmol L^{-1}, 5 mL), and o-phthalaldehyde (20 mg/1 mL methanol). The reaction solution (digestive juice: OPA reagent = 1: 20, v/v) was incubated at 37 °C for 2 min, and then the JH754PC spectrophotometre was employed to determine the absorbance at 340 nm.

2.12. Statistical analysis

Each measurement was repeated for at least three times. V.17.0 SPSS software (IBM Co., Chicago, USA) was used to analyse significant differences across data using Duncan's multiple comparisons at a

significance level of $p < 0.05$.

3. Results and discussion

3.1. Chemical constituent analysis of CERDFs

The degrees of substitution of the carboxymethyl and phosphate groups in CERDF-UDEC and CERDF-UDEPC were 3.52% and 1.19%, respectively. The IDF and total dietary fiber contents of CERDF were 63.82 and 68.81 g/100 g, respectively (Table 1), indicating that insoluble fiber was the major component of CERDF, consistent with the findings of Hanafi et al. (2022). Both CERDF-UDEC and CERDF-UDEPC showed lower IDF content and higher SDF contents compared to CERDF ($p < 0.05$). This was attributed to the degradation of hemicellulose and cellulose caused by dual enzymolysis and ultrasound (Zheng and Li, 2018). Ultrasound induce severe vibrations in polar molecules in the fibers, generating a cavitation effect (Zohaib et al., 2021). The grafting of carboxymethyl and phosphate onto CERDF increased its polarity, thereby enhancing the SDF content (Zheng et al., 2022). Moreover, CERDF-UDEC had a higher SDF content (18.65 g/100 g) which was approximately 2 times that of CERDF modified by cellulase hydrolysis and carboxymethylation (12.67 g/100 g) ($p < 0.05$) (Liu et al., 2021), revealing that ultrasound effectively increased the hydrophilicity of CERDF. Furthermore, a lower SDF content was observed in CERDF-UDEPC than in CERDF-UDEC ($p < 0.05$), mainly because of the lower degrees of substitution of CERDF-UDEPC (Ma et al., 2022). Additionally, the fat and protein contents of CERDF decreased after composite modifications ($p < 0.05$), which was mainly ascribed to the severe vibration caused by ultrasound (Tian et al., 2024).

3.2. Surface area and colour analysis of CERDF

An increase in surface area can enhance the affinity of DFs for water or oil, which is helpful for improving the textural properties of hydrogels (Farahani et al., 2023a; Jiang et al., 2020). After composite modifications, CERDF showed a smaller particle size ($D_{3,2}$) (Table 1), which was ascribed to the degradation of fiber chains resulting from ultrasound, cellulase, and hemicellulase hydrolysis (Zheng and Li, 2018). A previous study demonstrated that enzymatic hydrolysis increased the surface area of CERDF (Zheng et al., 2021). Compared to CERDF, CERDF-UDEC and CERDF-UDEPC showed considerable colour difference (ΔE) characterised by reduced L (representative of lightness) and increased a value (indicative of redness) ($p < 0.05$), indicating that ultrasound and dual enzymolysis combined with carboxymethylation or crosslinking took a negative effect on the lightness of CERDF. During these modifications, the degradation of natural pigments and browning reactions occur (Kanwar et al., 2023). Previous studies have shown that the addition of brown DFs can reduce the light transmittance of hydrogels and thus increase their anti-photooxidation abilities (Farahani et al., 2024b; Hou et al., 2022).

Table 1
Influences of different dual modifications on the chemical constitute, surface area, colour, and hydration properties of coconut endosperm residue dietary fiber.

Proximate Composition	CERDF	CERDF-DEC	CERDF-DEPC
Moisture (g•100 g^{-1})	5.97 ± 0.06c	5.145 ± 0.16c	4.94 ± 0.22c
Fat (g•100 g^{-1})	3.08 ± 0.12c	1.97 ± 0.11d	1.22 ± 0.07d
Ash (g•100 g^{-1})	1.74 ± 0.05c	1.99 ± 0.12c	2.16 ± 0.23c
Protein (g•100 g^{-1})	4.55 ± 0.14c	2.64 ± 0.23d	2.68 ± 0.25d
Total fiber (g•100 g^{-1})	68.81 ± 4.19d	87.73 ± 5.27c	87.29 ± 3.44c
Insoluble fiber (g•100 g^{-1})	63.82 ± 3.15d	69.08 ± 3.34c	72.85 ± 0.49c
Soluble fiber (g•100 g^{-1})	4.99 ± 0.08e	18.65 ± 1.46c	14.44 ± 0.96d
$D_{3,2}$ (μm)	142.36 ± 5.06c	103.58 ± 4.36e	114.32 ± 7.46d
Specific surface area (cm^2/cm^3)	1926.37 ± 4.54e	2857.48 ± 9.68c	2015.22 ± 9.68d
L	64.99 ± 3.45c	54.56 ± 0.46d	57.75 ± 0.38d
a	6.60 ± 0.20d	8.39 ± 0.31c	6.99 ± 0.42d
b	9.19 ± 1.46e	11.99 ± 0.34c	10.89 ± 0.37de
ΔE	Control	8.69	6.46
Water-holding ability (g/g)	6.86 ± 0.24e	16.48 ± 0.57c	12.99 ± 1.25d
Water-expansion ability (mL/g)	4.60 ± 0.40d	8.80 ± 0.20c	7.80 ± 0.20c
Viscosity (cP)	7.33 ± 0.94d	16.49 ± 1.43c	16.08 ± 0.47c

Data are mean ± standard deviation from triplicate determinations. CERDF, coconut endosperm residue dietary fiber; CERDF-DEC, CERDF modified by cellulase and hemicellulase hydrolysis united with carboxymethylation; CERDF-DEPC, CERDF modified by cellulase and hemicellulase hydrolysis combined with phosphate crosslinking; TDF, total dietary fiber; SDF, soluble dietary fibre; IDF, insoluble dietary fiber. $D_{3,2}$, the Sauter mean diameter of CERDFs. Colour indexes including L, a, and b are reprehensive of rightness, redness and yellowness of fibres, respectively, and ΔE means the difference in colour between CERDF and the modified CERDFs. Different lowercase letters (c–e) in the same row indicate significant difference ($p = 0.03$).

3.3. Structural analysis of CERDF

3.3.1. Surface microstructure

Fig. 1A and C show the changes in the microstructure of CERDF after the two composite modifications. CERDF exhibited a microstructure typical of fibers containing multiple cellulose tubes and debris (Fig. 1A). In contrast, a distinctly fragmented microstructure with greater porosity or more debris was observed in CERDF-UDEC and CERDF-UDEPC (Fig. 1B and C), mainly resulting from the breakdown of glycosidic linkages induced by ultrasound, dual-enzymatic hydrolysis, and alkali treatment during carboxymethylation (Kanwar et al., 2023). Moreover, the increased porosity and debris were predominantly attributed to the larger surface area (Table 1), which can enhance the interactions of fibers with water or egg white proteins, thus improving the textural properties of the hydrogels (Ma et al., 2022).

3.3.2. Fourier-transform infrared spectra

The FT-IR spectra of CERDF, CERDF-UDEC, and CERDF-UDEPC all contained typical peaks of fibres at 3345, 2900, 1620 and 1080 cm^{-1} (Fig. 2) (Khemakhem et al., 2019). The changes in several characteristic peaks revealed that the composite modifications altered the chemical bonds and functional groups of the CERDF. The peak at 3406 cm^{-1} in the spectrum of CERDF, which represented the asymmetric stretching of O–H, separately transferred to 3385 and 3379 cm^{-1} in the spectra of CERDF-UDEC and CERDF-UDEPC, suggesting the degradation of hydrogen bonds OF CERDF after ultrasound and dual enzymolysis combined with carboxymethylation or crosslinking (Ma et al., 2022). The new absorption peaks at 912 and 906 cm^{-1} in the spectra of CERDF-UDEC and CERDF-UDEPC, respectively, indicated the breakdown of β-glycosidic linkages caused by ultrasound and dual enzymolysis (Zheng and Li, 2018). In spectrum of CERDF-UDEPC, adsorption peaks in 1390 cm^{-1} (indicating the deformation of P = O bond) and 1518 cm^{-1} (representing the vibration of C–H) confirmed the successfully grafting of phosphate groups on CERDF (Jiang et al., 2020). Compared to CERDF, the wavenumber shifts at 1731 and 1159 cm^{-1} (representative stretching of methyl and carboxyl groups, respectively) in the spectrum of CERDF-UDEC suggest that carboxymethyl groups were grafted onto CERDF (Ma et al., 2022).

3.4. Hydration properties of CERDFs

CERDF-UDEC and CERDF-UDEPC exhibited higher WHA and WEA values than CERDF ($p < 0.05$) (Table 1). The improvements in the WHA and WEA of CERDF after ultrasound and dual enzymolysis separately combined with carboxymethylation and crosslinking were predominantly attributed to (1) the more porous and fragmented microstructure of CERDF (Fig. 1) and the larger surface area (Table 1), which enhanced the affinity between water and CERDF; and (2) the grafting of

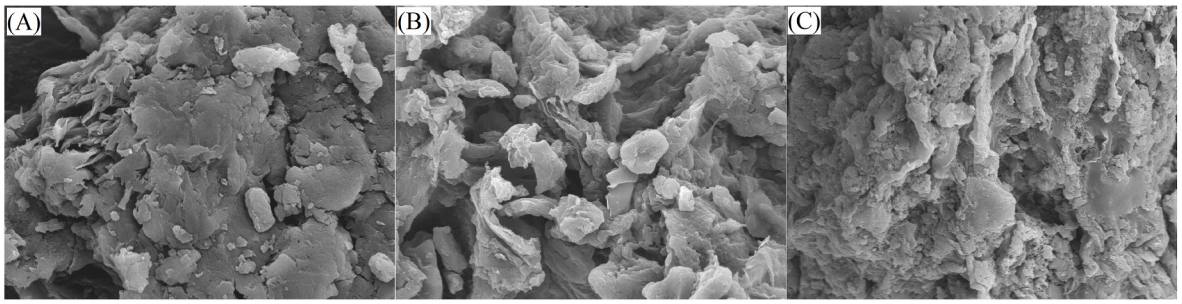

Fig. 1. Scanning electron micrographs of CERDF (A), CERDF-UDEC (B), and CERDF-UDEPC (C) with a magnification of 5000 × , at 5.0 kV and 1 μm. CERDF, millet bran dietary fiber; CERDF-UDEC, CERDF modified by ultrasound and dual enzymolysis combined with carboxymethylation; and CERDF-UDEPC, CERDF modified by ultrasound and dual enzymolysis combined with crosslinking.

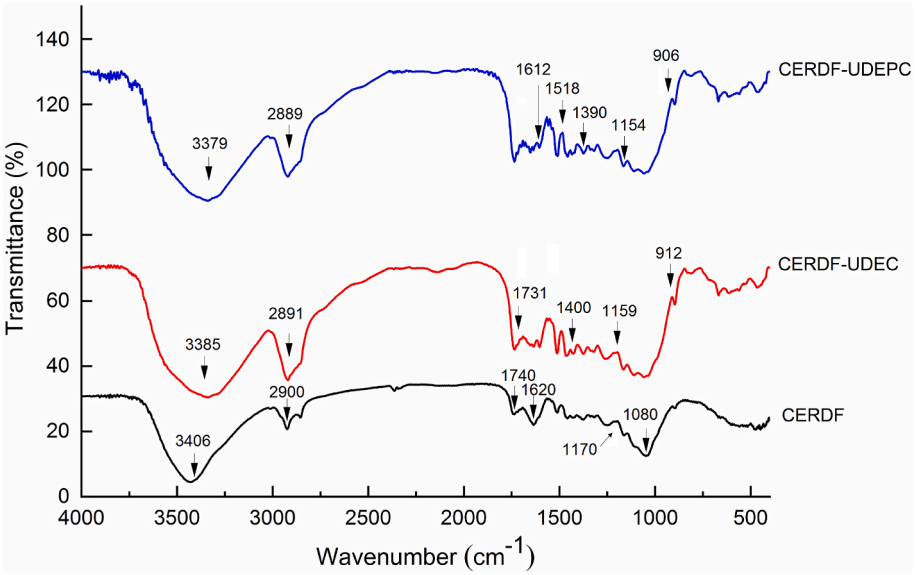

Fig. 2. Fourier-transformed infrared spectra of CERDF, CERDF-UDEC, and CERDF-UDEPC with a resolution of 4 cm^{-1} and wavenumber scanning range of 4000–400 cm^{-1}.

carboxymethyl and phosphate groups on CERDF, which increased its hydrophilicity (Ma et al., 2022). Moreover, the reasons for the high WHA and WSA of CERDF-UDEPC can be attributed to the network structure formed between the fiber chains after phosphate crosslinking, which allows it to retain more water molecules (Hazarika and Sit, 2016). The high WSA of CERDF-UDEA is consistent with its large surface area (Table 1) (Zheng and Li, 2018).

High solution viscosity is a prerequisite for polymers to form a gel formation (Zang et al., 2023). The viscosities of CERDF-UDEC and CERDF-UDEPC were higher than that of CERDF ($p < 0.05$) (Table 1), in accordance with their larger surface area, higher WHA, SDF content, and WEA, as well as their more porous or multichip microstructure (Table 1 and Fig. 1B–C). An improvement in the SDF content means that more fibers can contribute to the viscosity of the aqueous solution, whereas increases in the WHA, WEA, and surface area indicate that the interactions of fibers with water are stronger, enhancing the viscosity of the CERDF (Xu et al., 2023). Moreover, the viscosity of CERDF-UDEC was higher than carboxymethylated CERDF and cellulase hydrolysed CERDF (14.85 and 12.76 cP, respectively) (Zheng et al., 2021), highlighting that a combination of ultrasound, dual enzymolysis and carboxymethylation was more effective to increase viscosity of CERDF than any single modification.

3.5. Structural characteristics of EWPG

3.5.1. Surface microstructure

Scanning electron micrographs of EWPG and EWPGs fortified with 5 g/100 g CERDF (EWPG/CERDF), CERDF-UDEPC (EWPG/CERDF-UDEPC), or CERDF-UDEC (EWPG/CERDF-UDEC) are shown in Fig. 3A and D, respectively. EWPG had a smooth microsurface (Fig. 3A); whereas EWPG/CERDF, EWPG/CERDF-UDEPC, and EWPG/CERDF-UDEC had rough and granular microstructures with many tiny pores (Fig. 3B–F). During the preparation of heat-induced gels, dietary fiber can provide a skeleton on which egg white proteins can aggregate, which is helpful for the formation of three-dimensional microstructures with tiny holes (Zhao et al., 2023). Moreover, the skeletal structure of the fiber matrix can enhance interactions between egg white proteins and promote their adsorption onto the surface of gels, resulting in a granular surface microstructure (Ullah et al., 2019). Compared with the microstructure of EWPG/CERDF (Fig. 3B), the microstructures of EWPG/CERDF-UDEPC and EWPG/CERDF-UDEC were denser and more granular with smaller tiny holes (Fig. 3C–F), mainly due to their higher WEA and viscosity (Table 1) (Khemakhem et al., 2019).

Fig. 3D–F show the micrographs of EWPGs fortified with CERDF-UDEC at addition level of 1, 3, and 5 g/100 g, respectively. The microstructure of EWPG became progressively denser and more granular as the CERDF-UDEC addition increased. These findings align with the reports that high fibers concentration enhance the intramolecular

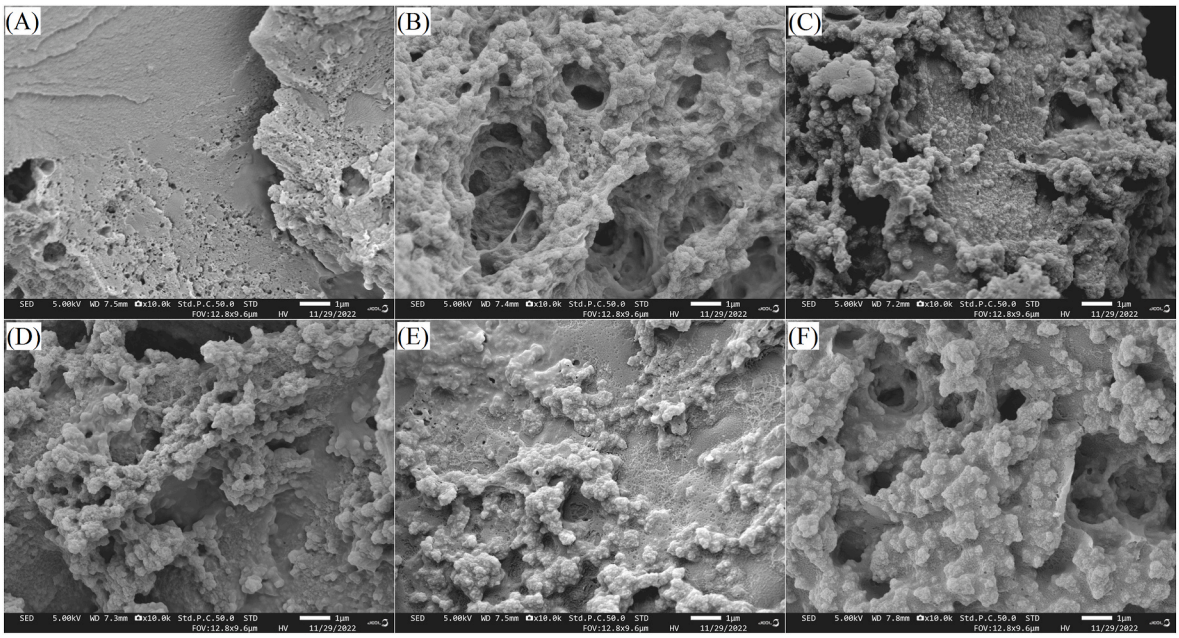

Fig. 3. Scanning electron micrographs of egg white protein gel (A), egg white protein gel fortified with 5 g/100 g CERDF (B), egg white protein gel containing of 5 g/100 g CERDF-UDEPC (C), egg white protein gel containing of 5 g/100 g CERDF-UDEC (D); egg white protein gel containing of 3 g/100 g CERDF-UDEC (E), and egg white protein gel containing of 1 g/100 g CERDF-UDEC (F) with a magnification of 10,000 × , at 5.0 kV and 1 μm.

and intermolecular interactions between egg white proteins, promoting the formation of a denser gel structure (Xu et al., 2023).

3.5.2. Secondary structure

Fig. 4 illustrates the α-helix, β-sheet, β-turn, and random coil contents of EWPG and EWPGs fortified with CERDFs. Compared to EWPG, β-turn content of EWPG decreased ($p < 0.05$), while β-sheet and random coil contents increased following the addition of CERDF, CERDF-UDEC, or CERDF-UDEPC. During heat-induced gels formation, egg white proteins unfold at elevated temperature increases following the stretched polypeptide chains aggregate into a three-dimensional spatial structure through hydrogen bonds or hydrophobic forces with decreasing temperature (Lee et al., 2024). The addition of CERDFs which exhibit substantial WHA and WEA (Table 1) enhanced the interactions of egg white proteins with water and expanded the structure of egg white proteins, leading to a denser and more granular gel. This facilitated the formation of β-sheet and random coil (Xu et al., 2023). Hydrogen bonding, a force maintaining the β-sheet of proteins. The carboxymethyl groups in CERDF-UDEC and the phosphate groups in CERDF-UDEPC were both further promoted the formation of hydrogen bonds between egg white proteins, facilitating the formation of β-sheets in EWPG (Xiao et al., 2020).

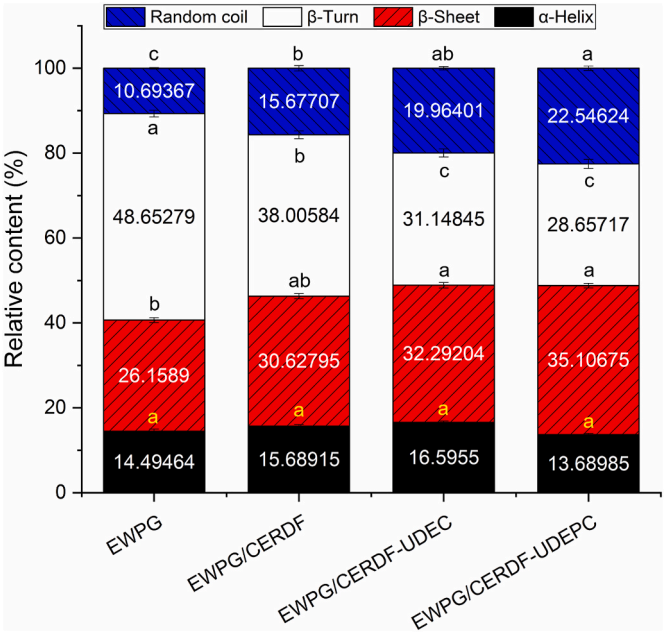

Fig. 4. Relative content of protein secondary structure of heat-induced egg white gels fortified with CERDFs at addition amount of 5 g/100 g. EWPG, heat-induced egg white protein gel; EWPG/CERDF, egg protein white protein gel with CERDF; EWPG/UDEC, egg white protein gel containing of CERDF-UDEC; and EWPG/UDEPC, egg white protein gel with CERDF-UDEPC. Data are mean ± standard deviation from triplicate determinations. Different lower letters (a–c) on the bars mean significant difference ($p = 0.03$).

3.6. Physicochemical properties of EWPG

3.6.1. WHA of EWPG

CERDF, CERDF-UDEC, and CERDF-UDEPC (3–5 g/100 g) demonstrated a dose-dependent improvement in the WHA of EWPG ($p < 0.05$) (Fig. 5A), mainly because of the considerable WHA of these CERDFs (6.86–16.48 g/g, Table 1) which increased the affinity of egg white proteins for water (Liu et al., 2022; Farahani et al., 2023b). Additionally, the incorporation of these CERDFs increased the random coil content in EWPGs (Fig. 4) and the number of tiny pores in the microstructure (Fig. 3B–D), which are beneficial for the unfolding of the gel structure and interactions between EWPGs and water molecules (Ullah et al., 2019). Furthermore, CERDF-HDEC (3–5 g/100 g) exhibited the highest ability to improve the WHA of H-EWG, mainly because of its high SDF content and WHA (Table 1), and its granular microstructure with many tiny holes (Fig. 3D), which facilitated superior water retention.

3.6.2. The pH of EWPG

At the isoelectric point, interactions between egg white proteins are minimal, resulting in a weak EWPG structure. Increasing in pH of EWPG can improve its WHA and textural properties (Manzoor et al., 2022). As shown in Fig. 5B, the pH of EWPG was 5.36, which was close to the

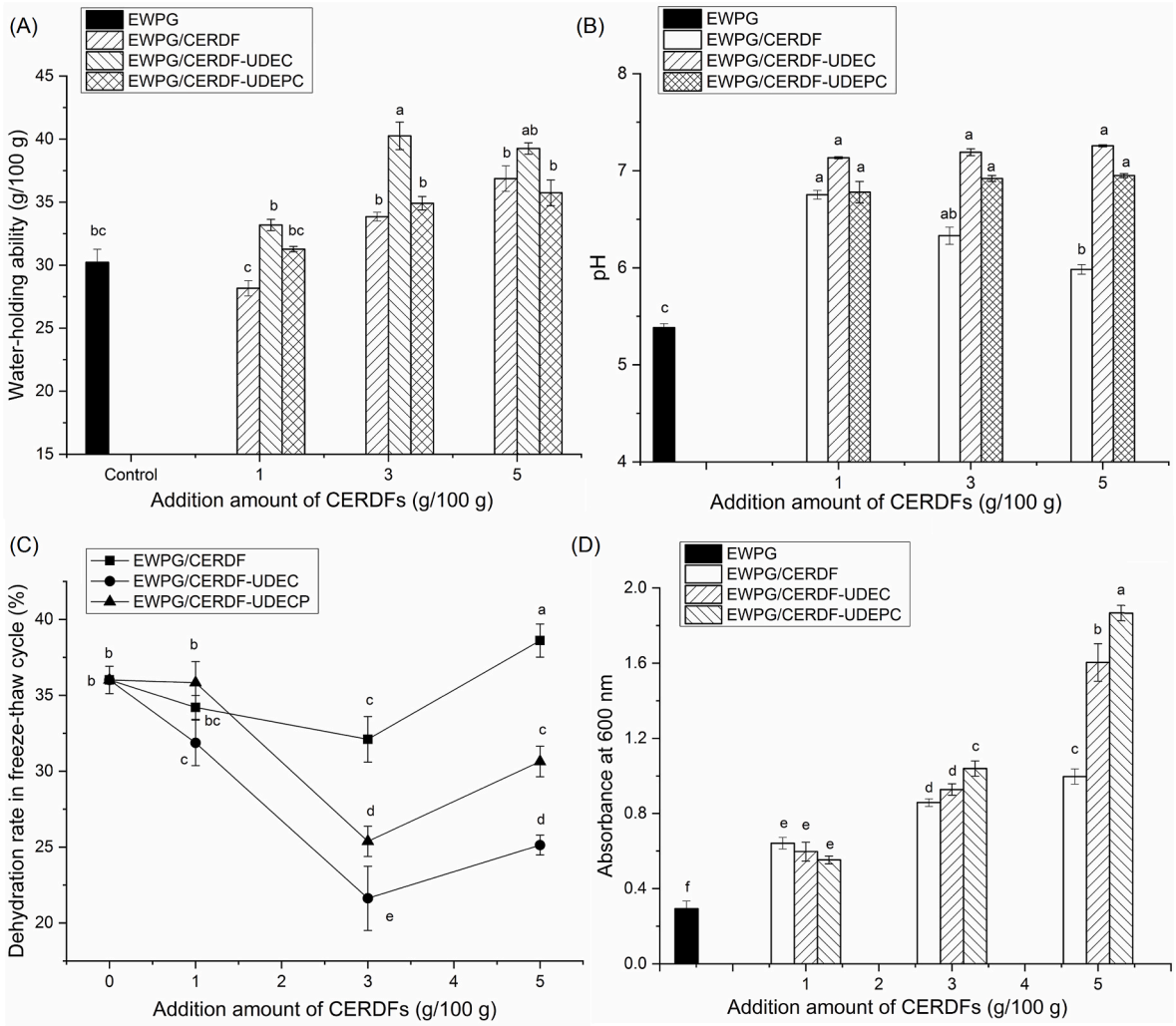

Fig. 5. Influence of different addition amount of CERDF, CERDF-UDEC, and CERDF-UDEPC on the water-holding ability (A), pH (B), dehydration rate in freeze-thaw cycle (C), and optical transparency (D) of egg white protein gel (EWPG). Data are mean ± standard deviation from triplicate determinations. Different lower letters (a–f) near the lines or on the bars mean significant difference ($p = 0.03$). The test parameters are as follows: the trigger force, compression rate, and test, pre-test, and post-test speeds were 5 g, 50%, 1, 2, and 1 mm/s, respectively.

isoelectric point of egg white protein (Xiao et al., 2020). Meanwhile, the pH value of EWPG was increased to approximately pH 7.0 after addition of CERDF, CERDF-UDEC, and CERDF-UDEPC at 3–5 g/100 g ($p < 0.05$). Previous studies have shown that a dense gel with a continuous network structure forms between egg white proteins at approximately pH 7.0 (Zang et al., 2023; Khemakhem et al., 2019). Therefore, the increased pH value was one reason for the improved effect of CREDFs on the microstructure and WHA of EWPG (Fig. 3B–D and Fig. 5A).

3.6.3. Dehydration rate under freeze-thaw cycle

During the freeze-thaw cycle, freezing induces the formation of a honeycomb-like gel structure with embedded ice crystal. As temperature rises, the ice crystals melt, separating the gel and water molecules, and creating water evolution channels, which result in dehydration, hardening, and shrinkage of the gels (Farahani et al., 2022b). A reduction in the dehydration rate of hydrogels during freeze-thaw cycles can help prevent these adverse effects (Bashash et al., 2022). The addition of CERDF, CERDF-UDEC, or CERDF-UDEPC decreased the dehydration rate of EWPG at 3–5 g/100 g ($p < 0.05$, Fig. 5C), demonstrating their effectiveness in mitigating gel deterioration during the freeze-thaw cycle. These CERDFs enhanced the microstructure and WHA of EWPG (Fig. 3B–D and Fig. 5A), and increased its β-sheet content (Fig. 4), resulting in a stronger affinity with water molecules under freeze-thaw cycle (Ma et al., 2022). Moreover, CERDF-UDEC and CERDF-UDEPC exhibited a more pronounced effect in reducing the freeze-thaw dehydration rate of EWPG than CERDF ($p < 0.05$), which is attributed to the higher SDF content, WEA, WHA, and viscosity of CERDF-UDEC and CERDF-UDEPC (Table 1). Additionally, the reduction effects of CERDF, CERDF-UDEC, and CERDF-UDEPC on the dehydration rate of EWPG at 3 g/100 g were greater than those at 5 g/100 g ($p < 0.05$). The addition of CERDFs at 3 g/100 g enhanced egg white protein aggregation and densified the microstructure of EWPG (Fig. 3C–D), which was not conducive to water loss in the freeze-thaw cycle (Hou et al., 2022). However, when the addition increased to 5 g/100 g, a large number of fibers with lower polarity reduced the interactions between egg white proteins and loosened the structure of EWPG, promoting water loss from the gel after the freeze-thaw cycle (Ullah et al., 2019).

3.6.4. Optical transparency of EWPGs

As shown in Fig. 5D, the addition of CERDF, CERDF-UDEC, and CERDF-UDEPC increased the absorbance of EWPG at 600 nm, verifying their reduced influence on the optical transparency ($p < 0.05$). As shown in Fig. 5B and A, the pH value of EWPG increased, and the interactions between egg white proteins and water molecules improved with addition of CERDFs. This enhancement facilitated the formation of a molecularly homogeneous network with higher light scattering (Jiang

et al., 2020), resulting in reduced transparency. Moreover, the addition of CERDFs made the microstructure of the EWPG denser and more granular (Fig. 3B, C, and D), increasing the scattering of light and thus decreasing the transparency of the gels (Zhao et al., 2023). Furthermore, the hydrophobic that primarily form and maintain heat-induced gels, were likely weakened by CERDFs addition, contributing to reduced transparency of the gels (Han et al., 2022). The reduction in transparency with CERDF was lower than that of CERDF-UDEC and CERDF-UDEPC at 5 g/100 g ($p < 0.05$), probably due to CERDF's lower WHA (Fig. 5A). Conversely, CERDF-UDEPC showed the strongest capacity to reduce EWPG transparency at 5 g/100 g, mainly because of the enhanced influence of phosphate groups on crosslinking between egg white proteins (Zheng et al., 2021). A reduction in optical transparency may benefit the application of EWPG in the preservation of photosensitive foods (Lee et al., 2024).

3.7. Texture properties of EWPG

The addition of CERDF, CERDF-UDEC, and CERDF-UDEPC enhanced the hardness of EWPG at 3–5 g/100 g ($p < 0.05$) in a dose-dependent manner (Table 2). CERDFs provide carbon skeletons that facilitate proteins adsorption and aggregation, enhancing the crosslinking of proteins and gel network strength, resulting in increased hardness (Zhao et al., 2023; Farahani and Mousavi, 2023). Additionally, the more granular and denser microstructures of the EWPG/CERDFs composites with higher WHA (Fig. 3B–D and Fig. 5A) further contributed to increased hardness of the gels (Ullah et al., 2019). The highest hardness (222.38 g) was observed in EWPG/CERDF-UDEPC, followed by EWPG/CERDF-UDEC, primarily attributed to their high WHA and denser microstructure (Fig. 5A–3C–D). Additionally, the phosphate group in CERDF-UDEPC and the carboxymethyl group in CERDF-UDEC enhanced crosslinking between egg white proteins (Zheng et al., 2021), further increasing the hardness of EWPG.

The EWPG gumminess increased with the addition of CERDFs in a dose-dependent manner (Table 2). A gumminess of a gel represents the energy needed for semi-solid food to become stable and is positively correlated with its hardness, cohesiveness, and viscosity (Zang et al., 2023). The increased hardness of EWPG after addition of CERDFs is one reason for the higher gumminess. Moreover, the higher random coil content (Fig. 4) was another reason for the higher gumminess of EWPG fortified with CERDFs (Liu et al., 2022). The addition of CERDF-UDEPC (5 g/100 g) resulted in the highest improvement in gumminess of EWPG, which can be attributed to its superior hardness and viscosity (Fig. 5A and Table 1).

The chewiness of gels is defined as the product of gumminess and springiness (Farahani et al., 2023c). Therefore, the increased gumminess of EWPG was primary responsible for the improvement in its chewiness following the addition of CERDFs. Additionally, the rise in pH (Fig. 5B) and WHA of EWPG (Table 2) contributed to the formation of a three-dimensional structure with greater chewiness (Khemakhem et al., 2019). CERDF-HDEAG exhibited the greatest ability to enhance the chewiness of EWPG, consistent with its superior WHA and WEA (Table 1) and the positive effect on the hardness of EWPG (Table 2). Increases in hardness, chewiness, and gumminess suggest expanded potential applications for EWPG in food, biomedicine, and cosmetic industries (Manzoor et al., 2022).

In contrast, the cohesiveness and resilience of EWPG were both reduced ($p < 0.05$) by the addition of CERDF-UDEPC at 1–3 g/100 g. Cohesiveness reflects the tensile strength of the gels. Following the addition of CERDFs, hydrophobic interactions between protein molecules decreased (Xiao et al., 2020) while the pH, WHA, and hardness of EWPG increased (Fig. 5A and B, and Table 2), which collectively hindered the tight aggregation of proteins, resulting in lower cohesiveness (Lv et al., 2022; Xu et al., 2023). Resilience is the ability of a gel to resist deformation (Zang et al., 2023). H-EWP/MBDF-DEPC exhibited lower resilience compared to H-EWPG upon the addition of MBDF-UDEPC at 1–5 g/100 g ($p < 0.05$), predominantly due to its high hardness. Excessive hardness is not conducive to the resilience of gels (Farahani et al., 2022d). Additionally, the springiness, cohesiveness, and resilience of H-EWPG remained largely unchanged after the addition of CERDF or CERDF-UDEC ($p > 0.05$).

3.8. In vitro digestion of EWPGs

The simulated gastric and intestinal digestion of EWPGs fortified with MBDFs (1–5 g/100 g) are shown in Fig. 6A–B, respectively. As shown in Fig. 6A, a significant declining trend was observed in the gastric digestion of EWPGs after the addition of CERDF, CERDF-UDEC, or CERDF-UDEPC at 3–5 g/100 g ($p < 0.05$). During gastric digestion, the network structure of EWPG is destroyed and egg white proteins are released and then hydrolysed by pepsin to produce oligopeptides or free amino acids (Zang et al., 2023). The addition of CERDFs densified the microstructure of EWPG and increased its pH (Fig. 3B), hardness, chewiness, and gumminess (Table 2), thereby increasing its stability against gastric hydrolysis. Additionally, CERDFs can reduce the interactions between pepsin and egg white proteins, and slowing down the gastric digestion speed (Xiao et al., 2020). CERDF-UDEPC showed a greater reducing effect on the gastric digestion of EWPG than CERDF and CERDF-UDEC at 3–5 g/100 g ($p < 0.05$), perhaps because of the high hardness and gumminess of EWPG/CERDF-UDEPC (Huyst et al., 2022). The phosphate groups in CERDF-UDEPC can promote cross-linking between egg white proteins, thus increasing the hardness of EWPG and leading to higher gastric stability (Zang et al., 2023).

Furthermore, the addition of CERDF (3–5 g/100 g) and CERDF-UDEC (1–5 g/100 g) increased the intestinal digestion of EWPG (Fig. 6B) ($p < 0.05$), suggesting that they improved the intestinal bioaccessibility of EWPG. A possible reason for this is that the pH of EWPG increased and adhesiveness decreased after the addition of CERDF and CERDF-UDEC, which was helpful for the intestinal digestion of H-EWPG (Zhao et al., 2023). In contrast, CERDF-UDEPC significantly decreased the intestinal

Table 2
Effects of different addition amounts of modified coconut endosperm residue dietary fibers on the texture properties of egg white protein gel.

Gels	Amount (g/100 g)	Hardness (g)	Adhesiveness	Springiness	Cohesiveness	Gumminess	Chewiness (g)	Resilience
EWPG	0	109.87 ± 8.37f	−43.72 ± 1.08c	0.91 ± 0.01a	0.78 ± 0.02a	85.72 ± 8.09e	78.07 ± 6.96e	0.305 ± 0.01d
EWPG/CERDF	1	93.07 ± 5.08f	−26.22 ± 0.64a	0.92 ± 0.00a	0.79 ± 0.02a	73.80 ± 5.92f	68.19 ± 5.69ef	0.352 ± 0.010b
	3	125.58 ± 10.90e	−34.30 ± 0.72b	0.93 ± 0.01a	0.79 ± 0.02a	99.70 ± 5.46d	92.71 ± 5.40d	0.322 ± 0.000c
	5	93.07 ± 5.08f	−26.22 ± 0.64a	0.92 ± 0.00a	0.79 ± 0.02a	78.30 ± 2.95f	68.19 ± 5.69ef	0.352 ± 0.001b
EWPG/CERDF-UDEC	1	127.42 ± 10.42e	−35.93 ± 3.27b	0.92 ± 0.02a	0.79 ± 0.02a	101.40 ± 7.46d	93.79 ± 3.98d	0.333 ± 0.010c
	3	135.77 ± 12.74d	−49.83 ± 5.12d	0.89 ± 0.03a	0.81 ± 0.02a	110.85 ± 9.72d	99.78 ± 9.49cd	0.343 ± 0.010b
	5	191.31 ± 8.77b	−52.66 ± 2.42d	0.93 ± 0.01a	0.85 ± 0.02a	163.32 ± 9.39b	108.87 ± 5.63cd	0.390 ± 0.010a
EWPG/CERDF-UDEPC	1	84.22 ± 7.27g	−50.25 ± 2.71d	0.89 ± 0.01a	0.69 ± 0.02b	58.49 ± 1.13g	52.36 ± 4.88g	0.152 ± 0.010h
	3	124.91 ± 5.07e	−43.15 ± 3.99c	0.85 ± 0.03a	0.65 ± 0.02b	94.08 ± 3.65d	71.95 ± 3.69e	0.195 ± 0.020g
	5	222.38 ± 1.67a	−47.67 ± 1.71cd	0.95 ± 0.00a	0.62 ± 0.01b	181.82 ± 3.77a	172.13 ± 3.41a	0.255 ± 0.000f

Data are mean ± standard deviation from triplicate determinations. Different small letters (a–f) in the same column indicate significant difference ($p = 0.03$).

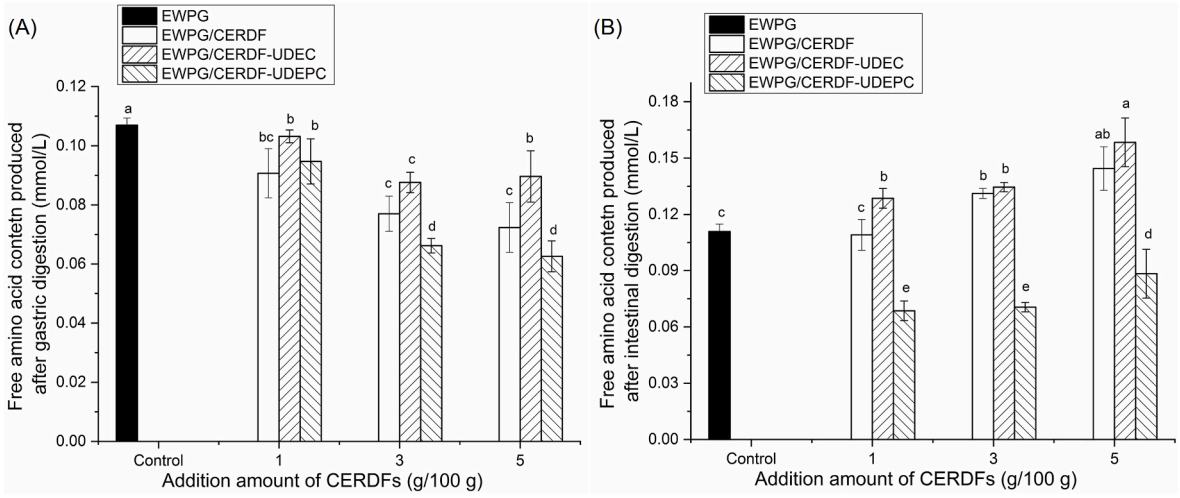

Fig. 6. Effects of different addition amount of CERDF, CERDF-UDEC, and CERDF-UDEPC on the gastric digestion (A) and intestinal digestion (B) of egg white protein gel. Data are mean ± standard deviation from triplicate determinations. Different lowercase letters (a–e) on the same type of column indicate significant difference ($p = 0.03$).

digestion of EWPG at 1–5 g/100 g, mainly due to the superior hardness of H-EWPG/CERDF-UDEPC (Table 2) (Farahani et al., 2024b). Gels can serve as carriers of active substances if they exhibit good stability against gastric digestion and high bioaccessibility in the small intestine (Bashash et al., 2022). Therefore, the addition of CERDF and CERDF-UDEC expands the application of EWPG as a bioactive carrier.

4. Conclusions

The hydrophilicity, surface area, WHA, viscosity, and WEA of CERDF were increased by ultrasound, cellulase, and hemicellulase hydrolysis combined with carboxymethylation or crosslinking. Compared to unmodified CERDF, CERDF-UDEC and CERDF-UDEPC more effectively improved EWPG properties, including water retention, pH, hardness, chewiness, and gumminess, while reducing freeze-thaw dehydration rate and transparency ($p < 0.05$). Additionally, adding CERDF and CERDF-UDEC improved the gastric stability and intestinal digestion of EWPG. These results indicate that ultrasound, cellulase, and hemicellulase hydrolysis, combined with carboxymethylation or crosslinking, are effective ways to improve the hydration properties of CERDF and the gel properties of EWPG. Further studies are required to investigate the mechanisms underlying of these modifications in CERDF and EWPG. Moreover, the safety and economic feasibility of these modifications across a broader range of food systems require additional investigation.

CRediT authorship contribution statement

Anyu Zhang: Investigation, Methodology, Writing – original draft. **Jun Ma:** Validation, Methodology, Writing-review. **Peiyao Long:** Data curation, Software, Writing – original draft. **Yajun Zheng:** Conceptualization, Writing – original draft, Funding acquisition. **Yichan Zhang:** Validation, Software, Writing-review.

Declaration of competing interest

The authors declare that they have no known competing financial interests or personal relationships that could have appeared to influence the work reported in this paper.

Acknowledgement

This work was supported by the Natural Science Foundation of Shanxi Province, China (202203021221139), and the Graduate practical innovation project of Shanxi Province, China (2024XSY77).

Data availability

Data will be made available on request.

References

Adeloye, J.B., Osho, H., Idris, L.O., 2020. Defatted coconut flour improved the bioactive components, dietary fibre, antioxidant and sensory properties of nixtamalized maize flour. J Agr. Food Res. 2, 100042. https://doi.org/10.1016/j.jafr.2020.100042.

Alavi, F., Emam-Djomeh, Z., Momen, S., Hosseini, E., Moosavi-Movahedi, A.A., 2020. Fabrication and characterization of acid-induced gels from thermally-aggregated egg white protein formed at alkaline condition. Food Hydrocolloids 99, 105337. https://doi.org/10.1016/j.foodhyd.2019.105337.

AOAC, 2000. Official Methods of Analysis. Association of Official Analytical Chemists, Washington, DC.

Bashash, M., Varidi, M., Varshosaz, J., 2022. Ultrasound-triggered transglutaminase-catalyzed egg white-bovine gelatin composite hydrogel: physicochemical and rheological studies. Innov. Food Sci. Energ., 102936 https://doi.org/10.1016/j.ifset.2022.102936.

Begum, F., Chutia, H., Bora, M., Deb, P., Mahata, C.L., 2024. Characterization of coconut milk waste nanocellulose based curcumin-enriched Pickering nanoemulsion and its application in a blended beverage of defatted coconut milk and pineapple juice. Int. J. Biol. Macromol., 129305 https://doi.org/10.1016/j.ijbiomac.2024.129305.

Church, F.C., Swaisgood, H.E., Porter, D.H., Catignani, G.L., 1983. Spectrophotometric assay using o-phthaldialdehyde for determination of proteolysis in milk and isolated milk Proteins1. J. Dairy Sci. 66, 1219–1227. https://doi.org/10.3168/jds.S0022-0302(83)81926-2.

Dong, R., Liao, W., Xie, J., Chen, Y., Peng, G., Xie, J., Sun, N., Liu, S., Yu, C., Yu, Q., 2022. Enrichment of yogurt with carrot soluble dietary fiber prepared by three physical modified treatments: microstructure, rheology and storage stability. Innov. Food Sci. Emerg. 75, 102901. https://doi.org/10.1016/j.ifset.2021.102901.

Farahani, Z.K., 2021. Halal edible biopolymers used in food encapsulation: a review. Journal of Human, Health and Halal Metrics 2, 52–56. https://doi.org/10.30502/jhhhm.2021.283062.1032.

Farahani, Z.K., Mousavi, M.E., 2023. Rheological behavior and textural characteristics resulting from the effect of different drying temperatures on the SFPG (soluble fraction of Persian gum). Food Chem. Adv 3, 100350. https://doi.org/10.1016/j.focha.2023.100350.

Farahani, Z.K., Mousavi, M., Ardebili, M.S., Bakhoda, H., 2022a. The effects of Ziziphus jujuba extract-based sodium alginate and proteins (whey and pea) beads on characteristics of functional beverage. J. Food Meas. Char. 16, 2782–2788. https://doi.org/10.1111/jfpp.17175.

Farahani, Z.K., Mousavi, M., Ardebili, S.M.S., Bakhoda, H., 2022b. Modification of sodium alginate by octenyl succinic anhydride to fabricate beads for encapsulating jujube extract. Curr. Res. Food Sci. 5, 157–166. https://doi.org/10.1016/j.crfs.2021.11.014.

Farahani, Z.K., Mousavi, S.M.A.E., Ardebili, S.M.S., Bakhoda, H., 2022c. Functional beverage based on alginate/insoluble fraction of Persian gum, WPI and PPC beads loaded with jujube extract: physicochemical, rheometry and sensory propertie. IJFST (Int. J. Food Sci. Technol.) 57, 499–505. https://doi.org/10.1111/ijfs.15423.

Farahani, Z.K., Mousavi, M., Ardebili, M.S., Bakhoda, H., 2022d. The influence of sodium alginate and sodium alginate/WPI as coating material on microcapsules of Jujube extract produced by spray dryer. J. Food Process. Preserv. 46, 17175. https://doi.org/10.1111/jfpp.17175.

Farahani, Z.K., Mousavi, M., Ardebili, M.S., Bakhoda, H., 2023a. Production and characterization of Ziziphus jujube extract-loaded composite whey protein and pea protein beads based on sodium alginate-IFPG (insoluble fraction of Persian gum). J. Sci. Food Agric. 103, 3674–3684. https://doi.org/10.1002/jsfa.12509.

Farahani, Z.K., Mousavi, M., Ardebili, M.S., Bakhoda, H., 2023b. Stability, physicochemical, rheological and sensory properties of beverage containing encapsulated jujube extract with sodium alginate stabilized by sodium alginate and Gellan gum. Food Chem. Adv 2, 100195. https://doi.org/10.1016/j.focha.2023.100195.

Farahani, Z.K., Mousavi, S.M.A.E., Ardebili, S.M.S., Bakhoda, H., 2023c. Impact of drying methods on textural/rheological attributes of insoluble fraction of Persian gum. Food Chem. Adv 3, 100479. https://doi.org/10.1016/j.focha.2023.100479.

Farahani, Z.K., Mousavi, M.A.E., Ardebili, M.S., Bakhoda, H., Nafchi, A.M., Paidari, S., 2024a. Chemical modification of Na-alginate by octenyl succinic anhydride and its complex with whey protein isolate to encapsulate jujube extract: physicochemical, morphological, thermal and structural properties. J. Food Meas. Char. 18, 3987–3999. https://doi.org/10.1007/s11694-024-02470-5.

Farahani, Z.K., Mousavi, M.E., Ibrahim, S.A., 2024b. Improving physicochemical, rheometry and sensory attributes of fortified beverages using jujube alcoholic/aqueous extract loaded Gellan-Protein macrocarriers. Heliyon 10, 24518. https://doi.org/10.1016/j.heliyon.2024.e24518.

Gan, J., Xie, L., Peng, G., Xie, J., Chen, Y., Yu, Q., 2021. Systematic review on modification methods of dietary fiber. Food Hydrocolloids 119, 106872. https://doi.org/10.1016/j.foodhyd.2021.106872.

Gao, K., Liu, T., Zhang, Q., Wang, Y., Song, X., Luo, X., Ruan, R., Deng, L., Cui, X., Liu, Y., 2023. Stabilization of emulsions prepared by ball milling and cellulase treated pomelo peel insoluble dietary fiber: integrity of porous fiber structure dominates the stability. Food Chem., 138189 https://doi.org/10.1016/j.foodchem.2023.138189.

Grootaert, C., Monge-Morera, M., Delcour, J.A., Skirtach, A.G., Rousseau, F., Schymkowitz, J., Dewettinck, K., Van der Meeren, P., 2022. Impact of heat and enzymatic treatment on ovalbumin amyloid-like fibril formation and enzymeinduced gelation. Food Hydrocolloids 131, 107784. https://doi.org/10.1016/j.foodhyd.2022.107784.

Han, T.F., Xue, H., Hu, X.B., Li, R.L., Liu, H.L., Tu, Y.G., Zhao, Y., 2022. Combined effects of NaOH, NaCl, and heat on the gel characteristics of duck egg white. LWT–Food Sci. Technol. 159, 113178. https://doi.org/10.1016/j.lwt.2022.113178.

Hanafi, F.N.A., Kamaruding, N.A., Shaharuddin, S., 2022. Influence of coconut residue dietary fiber on physicochemical, probiotic (Lactobacillus plantarum ATCC 8014) survivability and sensory attributes of probiotic ice cream. LWT–Food Sci. Technol. 154, 112725. https://doi.org/10.1016/j.lwt.2021.112725.

Hazarika, B.J., Sit, N., 2016. Effect of dual modification with hydroxypropylation and cross-linking on physicochemical properties of taro starch. Carbohydr. Polym. 140, 269–278. https://doi.org/10.1016/j.carbpol.2015.12.055.

Hou, Y., Liu, H., Zhu, D., Liu, J., Zhang, C., Li, C., Han, J., 2022. Influence of soybean dietary fiber on the properties of konjac glucomannan/κ-carrageenan corn oil composite gel. Food Hydrocolloids 129, 107602. https://doi.org/10.1016/j.foodhyd.2022.107602.

Huyst, A.M.R., Deleu, L.J., Luyckx, T., Van der Meeren, L., Housmans, J.A.J., Iqbal, S., Tirpanalan-Staben, Ö., Franke, K., 2022. Modification of dietary fibers to valorize the by-products of cereal, fruit and vegetable industry—a review on treatment methods. Plants 11, 3466. https://doi.org/10.3390/plants11243466.

Jiang, Y., Yin, H., Zheng, Y., Wang, D., Liu, Z., Deng, Y., Zhao, Y., 2020. Structure, physicochemical and bioactive properties of dietary fibers from Akebia trifoliata (Thunb.) Koidz. seeds using ultrasonication/shear emulsifying/microwave assisted enzymatic extraction. Food Res. Int. 136, 109348. https://doi.org/10.1016/j.foodres.2020.109348.

Kanwar, P., Yadav, R.B., Yadav, B.S., 2023. Influence of chemical modification approaches on physicochemical and structural properties of dietary fiber from oat. J. Cereal. Sci. 111, 103688. https://doi.org/10.1016/j.jcs.2023.103688.

Kar, A., Olenskyj, A.G., Guerrero, M.G., Graham, R., Bornhorst, G.M., 2023. Interplay of egg white gel pH and intragastric pH: impact on breakdown kinetics and mass transport processes. Food Res. Int. 173, 113290. https://doi.org/10.1016/j.foodres.2023.113290.

Khemakhem, M., Attia, H., Ayadi, M.A., 2019. The effect of pH, sucrose, salt and hydrocolloid gums on the gelling properties and water-retention ability of egg white gel. Food Hydrocolloids 87, 11–19. https://doi.org/10.1016/j.foodhyd.2018.07.041.

Lee, S., Jeong, S.K.C., Jeon, H., Kim, Y.J., Choi, Y.S., Jung, S., 2024. Heat-induced gelation of egg white proteins depending on heating temperature: insights into protein structure and digestive behaviors in the elderly in vitro digestion model. Int. J. Biol. Macromol. 262, 130053. https://doi.org/10.1016/j.ijbiomac.2024.130053.

Liu, Y., Yi, S., Ye, T., Leng, Y., Hossen, M.A., Sameen, D.E., Qin, W., 2021. Effects of superfine-grinding and homogenization on physicochemical properties of okara dietary fibers for 3D printing cookies. Ultrason. Sonochem. 77, 105693. https://doi.org/10.1016/j.ultsonch.2021.105693.

Liu, J.B., Chai, J.J., Yuan, Y.X., Zhang, T., Saini, R.K., Yang, M., Shang, X.M., 2022. Dextran sulfate facilitates egg white protein to form transparent hydrogel at neutral pH: structural, functional, and degradation properties. Food Hydrocolloids 122, 107094. https://doiorg/10.1016/j.foodhyd.2021.107094.

Lv, Y.Q., Wang, J., Xu, L.L., Tang, T.T., Su, Y.J., Gu, L.P., Chang, C.H., Zhang, M., Yang, Y.J., Li, J.H., 2022. Gel properties of okara dietary fiber-fortified soy protein isolate gel with/without NaCl. J. Sci. Food Agric. 103, 411–419. https://doi.org/10.1002/jsfa.12155.

Ma, Z., Yao, J., Wang, Y., Jia, J., Liu, F., Liu, X., 2022. Polysaccharide-based delivery system for curcumin: fabrication and characterization of carboxymethylated corn fiber gum/chitosan biopolymer particles. Food Hydrocolloids 125, 107367. https://doi.org/10.1016/j.foodhyd.2021.107367.

Manzoor, A., Dar, A.H., Pandey, V.K., Shams, R., Khan, S., Panesar, P.S., Kennedy, J.F., Fayaz, U., Khan, S.A., 2022. Recent insights into polysaccharide-based hydrogels and their potential applications in food sector: a review. Int. J. Biol. Macromol. 213, 987–1006. https://doi.org/10.1016/j.ijbiomac.2022.06.044.

Nansu, W., Ross, S., Ross, G., 2019. Mahasaranon, Effect of crosslinking agent on the physical and mechanical properties of a composite foam based on cassava starch and coconut residue fiber. Materialstody: Proceedings Roceedings 17, 2010–2019. https://doi.org/10.1016/j.matpr.2019.06.249.

Tan, Y.Y., Li, S.X., Liu, S.L., Li, C.F., 2022. Modification of coconut residue fiber and its bile salt adsorption mechanism: action mode of insoluble dietary fibers probed by microrheology. Food Hydrocolloids 136, 108221. https://doi.org/10.1016/j.foodhyd.2022.108221.

Tian, Y., Sheng, Y., Wu, T., Quan, Z., Wang, C., 2024. Effects of cavitation jet combined with ultrasound, alkaline hydrogen peroxide and Bacillus subtilis treatment on the properties of dietary fiber. Food Biosci. 59, 103895. https://doi.org/10.1016/j.fbio.2024.103895.

Trinidad, P.T., Mallillin, A.C., Valdez, D.H., Loyola, A.S., Askali-Mercado, F.C., Castillo, J.C., Encabo, R.R., Masa, D.B., Maglaya, A.S., Chua, M.T., 2006. Dietary fibre from coconut flour: a functional food. Innovat. Food Sci. Emerg. Technol. 7, 309–317. https://doi.org/10.1016/j.ifset.2004.04.003.

Ullah, I., Hu, Y., You, J., Yin, T., Xiong, S., Din, Z.U., Huang, Q.L., Liu, R., 2019. Influence of okara dietary fiber with varying particle sizes on gelling properties, water state and microstructure of tofu gel. Food Hydrocolloids 89, 512–522. https://doi.org/10.1016/j.foodhyd.2018.11.006.

Xiao, Y., Li, J., Liu, Y., Peng, F., Wang, X., Wang, C., Li, M., Xv, D., 2020. Gel properties and formation mechanism of soy protein isolate gels improved by wheat bran cellulose. Food Chem. 324, 126876. https://doi.org/10.1016/j.foodchem.2020.126876.

Xu, Y., Qi, J., Yu, M., Zhang, R., Lin, H., Yan, H., Li, C., Jia, J.M., Hu, Y., 2023. Insight into the mechanism of water-insoluble dietary fiber from star anise (Illicium verum Hook. f.) on water-holding capacity of myofibrillar protein gels. Food Chem. 423, 136348. https://doi.org/10.1016/j.foodchem.2023.136348.

Zang, J., Zhang, Y., Pan, X., Peng, D., Tu, Y., Chen, J., Zhang, Q.F., Tang, D.B., Yin, Z., 2023. Advances in the formation mechanism, influencing factors and applications of egg white gels: a review. Trends Food Sci. Technol. 138, 417–432. https://doi.org/10.1016/j.tifs.2023.06.025.

Zhao, X., Chen, B., Liu, T., Cai, Y., Huang, L., Zhao, M., Zhao, Q., 2023. The formation, structural and rheological properties of emulsion gels stabilized by egg white protein-insoluble soybean fiber complex. Food Hydrocolloids 134, 108035. https://doi.org/10.1016/j.foodhyd.2022.108035.

Zheng, Y.J., Li, Y., 2018. Physicochemical and functional properties of coconut (*Cocos nucifera* L) cake dietary fibres: effects of cellulase hydrolysis, acid treatment and particle size distribution. Food Chem. 257, 135–142. https://doi.org/10.1016/j.foodchem.2018.03.012.

Zheng, Y.J., Tian, H.L., Li, Y., Wang, X., Shi, P.Q., 2021. Effects of carboxymethylation, hydroxypropylation and dual enzyme hydrolysis combination with heating on physicochemical and functional properties and antioxidant activity of coconut cake dietary fibre. Food Chem. 336, 127688. https://doi.org/10.1016/j.foodchem.2020.127688.

Zheng, Y.J., Xu, B.F., Shi, P.Q., Tian, H.L., Li, Y., Wang, X.Y., Wu, S., Liang, P.F., 2022. The influences of acetylation, hydroxypropylation, enzymatic hydrolysis and crosslinking on improved adsorption capacities and in vitro hypoglycemic properties of millet bran dietary fibre. Food Chem. 368, 130883. https://doi.org/10.1016/j.foodchem.2021.130883.

Zohaib, H., Muhammad, I., Haseeb, A.M., Kamran, K.M., 2021. Ultrasound-Assisted modification of insoluble dietary fiber from chia (salvia hispanica L.) seeds. J. Food Qual. https://doi.org/10.1155/2021/5035299.